

Room-temperature perpendicular magnetic anisotropy of Pt/Co/AlO_x trilayers on SrTiO₃ (001)

Cite as: AIP Advances **10**, 105010 (2020); <https://doi.org/10.1063/5.0023282>

Submitted: 28 July 2020 . Accepted: 14 September 2020 . Published Online: 06 October 2020

Ye Du , Shoma Arai, Shingo Kaneta-Takada, Le Duc Anh, Shutaro Karube , Makoto Kohda, Shinobu Ohya , and Junsaku Nitta

COLLECTIONS

Paper published as part of the special topic on [Chemical Physics](#), [Energy, Fluids and Plasmas](#), [Materials Science](#) and [Mathematical Physics](#)



View Online



Export Citation



CrossMark

AIP Advances Nanoscience Collection

READ NOW!

Room-temperature perpendicular magnetic anisotropy of Pt/Co/AlO_x trilayers on SrTiO₃ (001)

Cite as: AIP Advances 10, 105010 (2020); doi: 10.1063/5.0023282

Submitted: 28 July 2020 • Accepted: 14 September 2020 •

Published Online: 6 October 2020



Ye Du,^{1,2} Shoma Arai,³ Shingo Kaneta-Takada,³ Le Duc Anh,^{3,4,5} Shutaro Karube,^{1,6} Makoto Kohda,^{1,2,6,7,a)} Shinobu Ohya,^{3,4,8,a)} and Junsaku Nitta^{1,2,6,a)}

AFFILIATIONS

¹Department of Materials Science, Tohoku University, Sendai 980-8579, Japan

²Center for Science and Innovation in Spintronics, Tohoku University, Sendai 980-8577, Japan

³Department of Electrical Engineering and Information Systems, The University of Tokyo, Bunkyo, Tokyo 113-8656, Japan

⁴Institute of Engineering Innovation, The University of Tokyo, Bunkyo, Tokyo 113-8656, Japan

⁵PRESTO, Japan Science and Technology Agency, 4-1-8 Honcho, Kawaguchi, Saitama 332-0012, Japan

⁶Center for Spintronics Research Network, Tohoku University, Sendai 980-8577, Japan

⁷Division for the Establishment of Frontier Sciences, Tohoku University, Sendai 980-8577, Japan

⁸Center for Spintronics Research Network (CSRN), The University of Tokyo, Bunkyo, Tokyo 113-8656, Japan

^{a)} Authors to whom correspondence should be addressed: makoto@material.tohoku.ac.jp; ohya@cryst.t.u-tokyo.ac.jp; and nitta@material.tohoku.ac.jp

ABSTRACT

We demonstrate room-temperature perpendicular magnetic anisotropy (PMA) in Pt/Co/AlO_x trilayers sputter-deposited onto a SrTiO₃ (STO) (001) substrate. Reflection high-energy electron diffraction and x-ray diffraction results confirm the two-dimensional polycrystalline nature for both Pt and Co layers in PMA films, which are (111) oriented in the out-of-plane direction. While the PMA in Pt/Co/AlO_x trilayers on STO (001) is found to have interfacial origins, sizable PMA is maintained when Pt layer thickness is as thin as 1 nm, which is several times to one order of magnitude smaller than the reported values of the spin diffusion length for Pt, thus facilitating spin transmission along the thin-film-normal direction. With the STO (001) substrate serving as the fundamental building block for realizing giant Rashba spin splitting, this work provides a feasible platform for the investigation of magnetization switching in two-dimensional-electron-gas-based magnetic hetero-structures at room temperature.

© 2020 Author(s). All article content, except where otherwise noted, is licensed under a Creative Commons Attribution (CC BY) license (<http://creativecommons.org/licenses/by/4.0/>). <https://doi.org/10.1063/5.0023282>

Since the discovery of perovskite SrTiO₃/LaAlO₃ (STO/LAO) high-mobility two-dimensional electron gas (2DEG) by Ohtomo and Hwang,¹ various related physical phenomena have been discovered such as the 2D superconductivity,^{2,3} emergent ferromagnetism,⁴ and novel quantum magneto-transport.^{5,6} Over the past few years, STO-based perovskite hetero-structures have exhibited new functionalities in the research field of spintronics. In particular, gate-tunable Rashba spin-orbit coupling⁷ has been unveiled at the (001)-oriented STO/LAO interface, fostering very efficient

spin-charge current conversions observed later^{8–13} at both low temperature and room temperature in the presence of Rashba spin-orbit interaction.^{14,15} Such a large spin-charge conversion efficiency at oxide interfaces shows considerable potential in spintronic applications such as magnetization switching^{16,17} and spin-orbit-based logic operations.¹⁸

In view of spintronic applications based on the perovskite substrate [e.g., the STO (001) single-crystalline substrate that is commonly used^{1–6,8–13,19,20}], metallic hetero-structures with

room-temperature perpendicular magnetic anisotropy (PMA)²¹ are particularly favorable because they allow enhanced device density and thermal stability compared with the in-plane-magnetized ones. However, achieving room-temperature PMA in multilayer films prepared on a STO (001) substrate is challenging. For example, although PMA was found in a thin ferromagnetic Co layer sandwiched by the STO (001) substrate and a 2.4 nm Pt capping layer below 190 K,²² the PMA deteriorates at 300 K. In a very recent study, sizable PMA was successfully obtained in [Ni/Pt] (001) epitaxial superlattices by strain engineering,²³ but high temperature (400 °C) is required during the deposition process, which leads to undesirable interlayer atomic diffusion. Alternatively, it was reported that the deposition of a 5 nm amorphous CaTiO₃ buffer layer²⁴ beneath the Co/Pt bilayers dramatically promotes the room-temperature PMA of the stack. It suggests that the PMA can be enhanced by utilizing a proper buffer layer for the ferromagnet. Nevertheless, as an oxide layer, 5 nm CaTiO₃ is relatively thick, and diffusive spin current transmitting through it may decay rapidly. Therefore, up to now, a convenient way to obtain the room-temperature PMA in nanoscale films prepared on a STO (001) substrate with a thin, metallic buffer layer that facilitates spin transmission is lacking.

In this work, we demonstrate, for the first time, the room-temperature PMA in Pt/Co/AlO_x trilayers sputter-deposited onto a STO (001) substrate at ambient temperature. Detailed structural characterizations reveal the 2D polycrystalline nature²⁵ for both Pt and Co layers, which are oriented in the [111] out-of-plane direction (note that the term “2D polycrystalline” refers to structural properties and is not related to the quantum confinement such as that in 2D electron or hole gas^{1,19,20}). The PMA is maintained when Pt layer thickness is reduced to 1 nm, which is several times to one order of magnitude smaller than the reported values of the spin diffusion length for Pt,^{26,27} thus allowing efficient spin-current transmission. Our results provide a convenient method to achieve PMA on STO (001) at room temperature despite the different orientation symmetries between the substrate and the ferromagnet, i.e., a fourfold in-plane symmetry for STO (001), while a sixfold in-plane symmetry for Co (111).

Thin films of Pt (t_{Pt})/Co (t_{F})/AlO_x (2 nm) trilayers are sputter-deposited at ambient temperature onto a STO (001) substrate by using an ultrahigh-vacuum rf magnetron sputtering facility. All the layers are deposited with a sputtering power of 50 W under an Ar pressure ranging from 0.2 Pa to 0.7 Pa. Before the deposition, to obtain an atomically flat TiO₂-terminated surface on the substrate, it is chemically etched by buffered HF and annealed in an electrical furnace at 1000 °C for 1 h in the atmosphere. In addition to the films deposited onto STO (001), several sets of films are also prepared on a thermally oxidized Si substrate (Si/SiO_x) as control samples. The thicknesses of the layers are pre-determined using the conventional stylus measurement. Reflection high-energy electron diffraction (RHEED) and x-ray diffraction (XRD) are used to characterize the crystallinity of the samples. The magnetic anisotropy of the thin films is examined by using the polar magneto-optic Kerr effect (MOKE) measurement.

Figure 1 shows the RHEED patterns of each layer for Pt (1 nm)/Co (t_{F})/AlO_x (2 nm) thin films with (a) t_{F} = 0.3 nm, (b) t_{F} = 0.6 nm, and (c) t_{F} = 1.0 nm. The AlO_x layer is found to

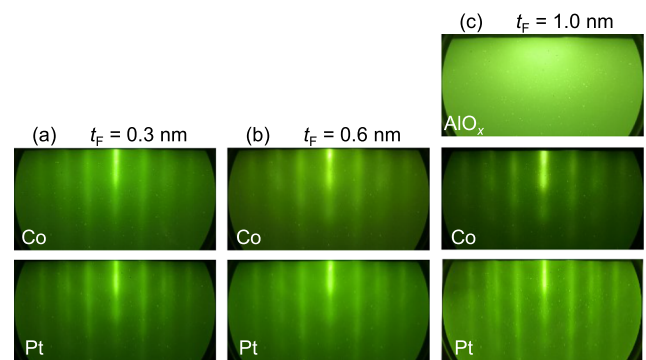


FIG. 1. Reflection high-energy electron diffraction patterns for Pt (1 nm)/Co (t_{F})/AlO_x (2 nm) thin films sputter-deposited onto STO (001) substrates with (a) t_{F} = 0.3 nm, (b) t_{F} = 0.6 nm, and (c) t_{F} = 1.0 nm. The AlO_x layer is amorphous for all of the samples. The incident electron beam direction is along STO [100].

be amorphous for all the samples. The Pt patterns are very different from those of (111)-oriented epitaxial Pt films²⁸ prepared on, e.g., an Al₂O₃ (0001) substrate but are highly consistent with a 2D polycrystalline description,²⁵ where all the Pt grains are (111) oriented in the film normal direction, while their in-plane orientations are highly randomized. This result seems to be natural because Pt, having a face-centered-cubic (fcc) structure, is expected to acquire the lowest surface energy²⁹ with crystals oriented in the close-packed {111} planes. As for the Co layer, as its RHEED patterns are almost identical to those of (111)-oriented Pt, it is suggested that Pt and Co layers have epitaxial relationship within each grain. In addition, Co is probably fcc instead of the hexagonal-close-packed (hcp) structure because the maximum t_{F} in our study (=1.0 nm) is less than 6–8 monolayers of (111) Co, above which thickness there occurs a phase transition from fcc to hcp, according to a previous study.³⁰

As shown in Fig. 2, the 2D polycrystalline nature of the Pt layer is further corroborated by using XRD characterizations. Figure 2(a) shows the out-of-plane XRD patterns for the 10 nm Pt layer deposited onto a STO (001) substrate and also for a bare substrate. From the comparison, it is confirmed that all the Pt grains are aligned along the [111] out-of-plane orientation. The in-plane XRD scan for the Pt (110) peak shown in Fig. 2(b) suggests that the in-plane orientations of Pt grains are highly randomized because no preferred orientations are found. This is also consistent with the description for a 2D poly-crystal.²⁵ It is worth noting that a 12-period oscillation appears in the in-plane XRD scan [Fig. 2(b)], indicating the existence of twin crystals for Pt (111) planes that have 30° offset with respect to each other [inset of Fig. 2(b)]. Nevertheless, the exact origin for such an oscillation is not yet clear, but it is likely to originate from the high symmetry of (111)-oriented Pt crystals on STO (001).

Figures 3(a)–3(g) show the polar MOKE results for Pt (1 nm)/Co (t_{F})/AlO_x (2 nm) thin films on STO (001) with t_{F} ranging from 0.3 nm to 1.0 nm. With increasing t_{F} , out-of-plane hysteresis opens a window in the t_{F} range of 0.41 nm–0.6 nm, suggesting sizable PMA of the trilayer thin films. With a further increase in t_{F} , the PMA vanishes as a result of overwhelming in-plane shape

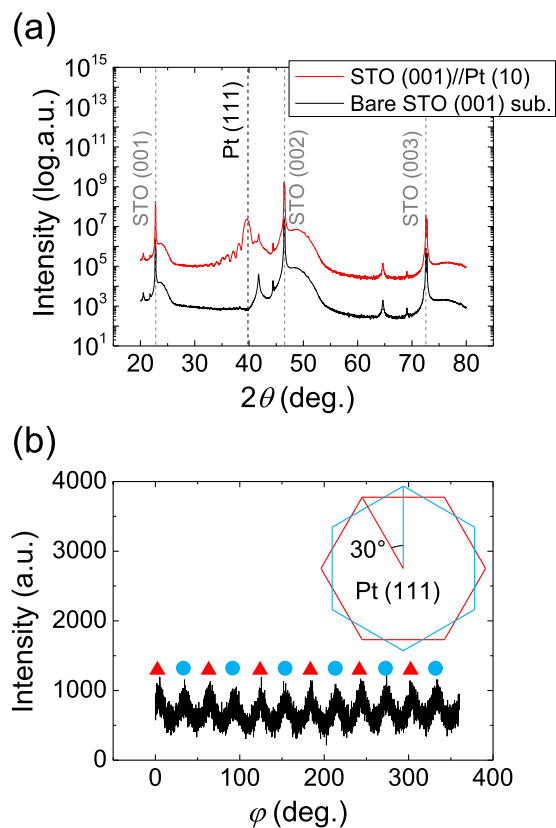


FIG. 2. (a) Out-of-plane x-ray diffraction patterns for a STO (001) substrate and for a 10 nm Pt thin film deposited onto STO (001). (b) In-plane x-ray diffraction patterns for the Pt (110) peak, suggesting the existence of 30°-offset twin crystals as shown in the inset.

anisotropy in the Co layer. Figure 3(h) shows the summary of the t_F dependence of coercivity for STO (001)-based samples and also for control samples of Si/SiO_x//Ta (1 nm)/Pt (1 nm)/Co (t_F)/AlO_x (2 nm) and Si/SiO_x//Ta (1 nm)/Pt (3 nm)/Co (t_F)/AlO_x (2 nm). The polar MOKE loops for thin films on Si/SiO_x are shown in Fig. 4. It clearly demonstrates that, with the introduction of 2D poly-crystal in Pt/Co/AlO_x trilayers, sizable PMA can be achieved with a thin Pt buffer layer of only 1 nm, while the PMA vanishes if the same layered thin films are deposited onto Si/SiO_x substrates with a 1 nm Ta buffer layer. This shows the distinct advantage of our 2D polycrystalline films to achieve PMA compared to conventional 3D polycrystalline films,^{31–33} where a thicker Pt buffer layer of, e.g., 3 nm, is required.

The PMA in Pt/ferromagnet/oxide trilayers has been found to have interfacial origins.^{30–32} The PMA of a ferromagnetic metal such as Co is strongly related to the anisotropy of its 3d orbitals. The orbital symmetry breaking by an interface results in an energy difference between 3d orbitals pointing toward the interface and pointing within the interfacial plane,³² which gives rise to PMA.³⁴ On one hand, it was demonstrated that the PMA can be dramatically enhanced via the hybridization at the Pt/ferromagnet

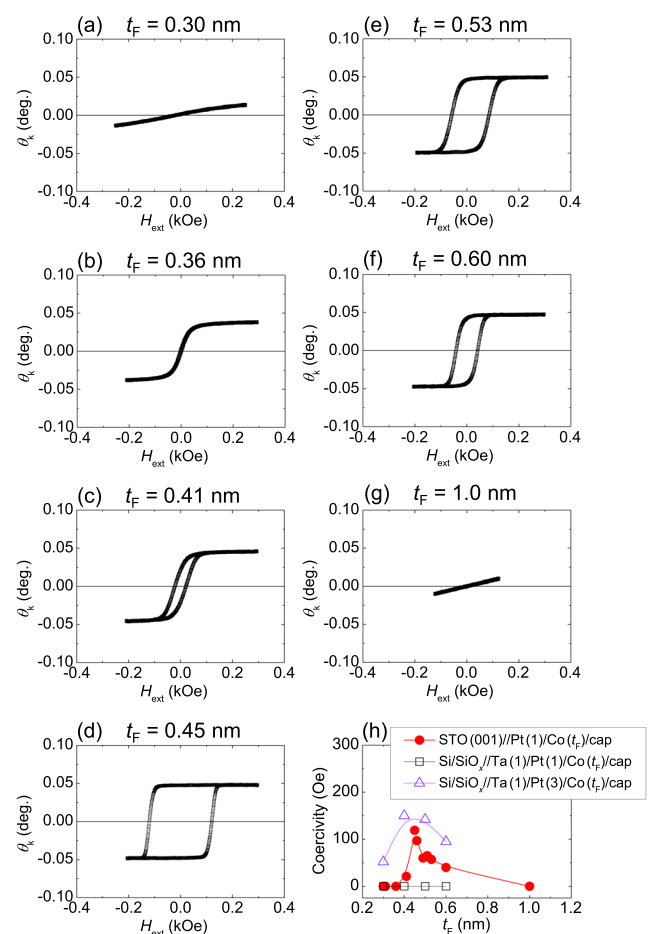


FIG. 3. (a)–(g) Polar MOKE results for STO (001)/Pt (1 nm)/Co (t_F)/AlO_x (2 nm) thin films with t_F ranging from 0.3 nm to 1.0 nm. (h) Co layer thickness t_F dependence of coercivity for STO (001)/Pt (1 nm)/Co (t_F)/cap, Si/SiO_x//Ta (1 nm)/Pt (1 nm)/Co (t_F)/cap, and Si/SiO_x//Ta (1 nm)/Pt (3 nm)/Co (t_F)/cap, where “cap” stands for 2 nm amorphous AlO_x.

interface.³⁰ On the other hand, the charge transfer³⁵ between the ferromagnet and oxygen atoms of the oxide layer (AlO_x, MgO *et al.*) has also been proposed to play a significant role because it can reduce the energy of the out-of-plane orbitals and thus increase the PMA.^{31–33,36}

As for a discussion on the origin of the PMA in our 2D polycrystalline thin films, it is demonstrated that the PMA disappears dramatically by replacing the capping layer from AlO_x to MgO [Fig. 5(a)], where the MgO capping layer, in contrast to the amorphous AlO_x capping layer, shows certain crystallinity [Fig. 5(b)]. This is clear evidence that the origin of PMA is strongly associated with the interfacial condition at the Co/oxide interface.³¹ Such a result is somewhat consistent with a previous study³⁶ that the PMA becomes rather weak in the as-deposited Pt/Co (0.6 nm)/MgO (2 nm) trilayers on Si/SiO_x without any post-annealing. It was previously shown that an optimized density of Co–O bonding is required

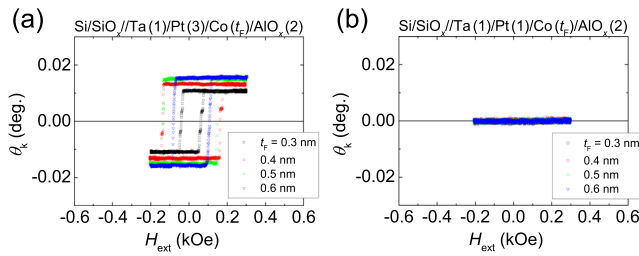


FIG. 4. Polar MOKE results of (a) Ta (1 nm)/Pt (3 nm)/Co (t_F)/AlO_x (2 nm) and (b) Ta (1 nm)/Pt (1 nm)/Co (t_F)/AlO_x (2 nm) thin films deposited at room temperature onto Si/SiO_x substrates.

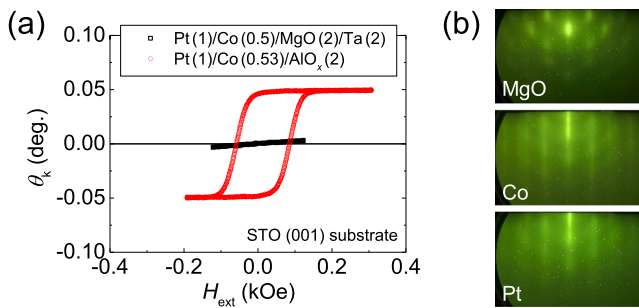


FIG. 5. (a) Polar MOKE results for Pt (1 nm)/Co (0.5 nm)/MgO (2 nm)/Ta (2 nm) and Pt (1 nm)/Co (0.53 nm)/AlO_x (2 nm) thin films deposited onto STO (001) substrates. (b) Reflection high-energy electron diffraction patterns for the Pt, Co, and MgO surface of the Pt (1 nm)/Co (0.5 nm)/MgO (2 nm)/Ta (2 nm) thin film.

to maximize the PMA,³² i.e., an either under-oxidized or over-oxidized Co layer leads to a reduced PMA.³⁷ This result indicates that in our samples, the Co/AlO_x interface with an amorphous AlO_x capping layer acquires a more optimized density of Co–O bonding compared to the Co/MgO interface with a crystallized MgO capping layer in favor of PMA.

Figures 6(a)–6(d) show that the PMA of Pt/Co/AlO_x trilayers drastically deteriorates when Pt buffer layer thickness reduces below 1 nm. This is accompanied by a gradual degradation of Co [111] orientation because, as a distinct comparison, a Co single layer deposited directly onto the STO (001) substrate becomes polycrystalline or amorphous [Fig. 6(e)], while a Co layer deposited upon the 1.0 nm Pt buffer layer is highly (111) oriented as shown in Fig. 1. It suggests that the [111] orientation in the Co layer is promoted by the (111)-oriented Pt buffer layer [Figs. 6(e)–6(h)]; additionally, such a [111] orientation is beneficial to obtaining a sizable PMA in Co, which is consistent with previous PMA studies in (111)-oriented Pt/Co superlattices, where an oxide capping layer is absent.^{30,38,39} It indicates that the Pt 5*d*–Co 3*d* hybridization³⁰ at the (111)-oriented Pt/Co interface contributes positively to the PMA in our samples.

The discussion above shows that the PMA in our 2D polycrystalline samples is intimately related to the oxidation condition

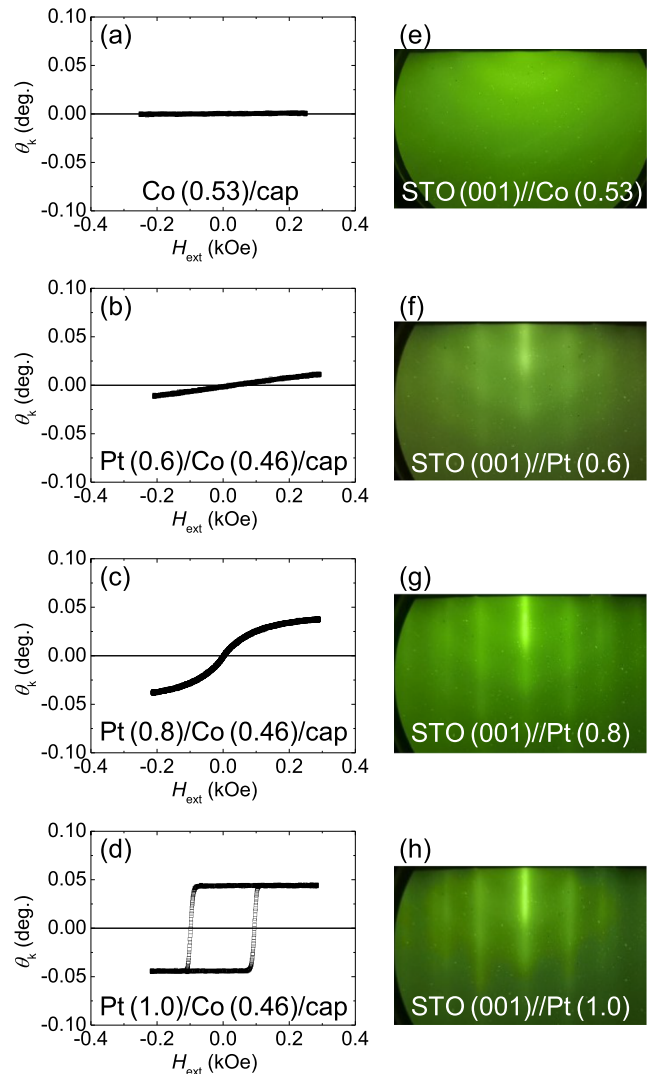


FIG. 6. Polar MOKE results for (a) Co (0.53 nm)/cap, (b) Pt (0.6 nm)/Co (0.46 nm)/cap, (c) Pt (0.8 nm)/Co (0.46 nm)/cap, and (d) Pt (1.0 nm)/Co (0.46 nm)/cap thin films deposited onto STO (001) substrates, where the “cap” stands for 2 nm AlO_x. Reflection high-energy electron diffraction patterns for (e) 0.53 nm Co, (f) 0.6 nm Pt, (g) 0.8 nm Pt, and (h) 1.0 nm Pt single-layer thin films deposited onto STO (001) substrates.

at Co/AlO_x interfaces; additionally, the observed PMA is likely to be associated with the strong Pt/Co interfacial hybridization, which occurs in the presence of Co (111).³⁰ Note that a recent study²³ suggests the interfacial strain effect to be another possible origin of PMA in Pt-based thin films deposited onto STO (001). As for our present study, the 12-period oscillation shown in Fig. 2(b) is clear evidence that the strain is not fully released, at least within the plane of the Pt/Co bilayers; additionally, a significant magnetic anisotropy difference is found when comparing the MOKE results of 2D polycrystalline films [solid circles, Fig. 3(h)] and conventionally 3D polycrystalline films [open

squares, Fig. 3(h)], where strong PMA is found for the former (with in-plane strain), but not for the latter (without in-plane strain). These structural and magnetic characterizations suggest a possible correlation between the strain effect and PMA in 2D polycrystalline thin films, but further studies are in need to verify such a correlation.

Our results show that PMA can be successfully obtained in Pt/Co/AlO_x trilayers prepared on a STO (001) substrate, where the Pt and Co layers are (111)-oriented 2D poly-crystals. Such a method to achieve PMA in a thin ferromagnetic Co layer can potentially be applied to other (001)-oriented perovskite oxides because of their similar lattice constants. This is very encouraging for spin-current-based applications such as 2DEG-based magnetization switching because conventional 2DEG built upon a STO (001) substrate requires another (001)-oriented epitaxial LAO oxide layer on top.^{8–10,12} Moreover, another merit of this work is the utilization of very thin Pt buffer layer, which facilitates efficient spin transmission. This is because the spin diffusion length of Pt is reported to be several times to one order of magnitude larger than such a buffer layer thickness (e.g., 1 nm),^{26,27} and thus, the spin relaxation effect within the Pt layer is expected to be negligible on the vertical spin transport. Thanks to such a merit, the spin current originating from the Rashba spin accumulation at the STO/LAO interface^{8–13} is expected to be efficiently absorbed by the neighboring ferromagnetic Co layer via the transfer of spin angular momentum.

In conclusion, we demonstrate room-temperature PMA in Pt/Co/AlO_x trilayers sputter-deposited onto STO (001) at ambient temperature, where Pt and Co layers are confirmed to be 2D poly-crystals with the [111] out-of-plane orientation. Sizable PMA is maintained when Pt buffer layer thickness is reduced to 1 nm, which is expected to be thin enough for efficient vertical spin transmission. Our results show that strong PMA can be achieved at room temperature, despite very different in-plane orientation symmetries between the STO (001) substrate and the ferromagnetic Co layer. Moreover, this work provides a convenient platform for the investigation of magnetization switching in 2DEG-based PMA hetero-structures at room temperature.

This work was partly supported by the Grants-in-Aid for Scientific Research by MEXT (Grant Nos. 18H03860 and 15H05699) and the Spintronics Research Network of Japan (Spin-RNJ). The authors would like to thank Professor Nobuki Tezuka for the help on the in-plane x-ray diffraction measurement. We also thank Professor Hitoshi Tabata and Professor Munetoshi Seki for technical support for the substrate treatment and Shu Kitamura and Daichi Sugawara for technical support on the MOKE measurement.

DATA AVAILABILITY

The data that support the findings of this study are available from the corresponding author upon reasonable request.

REFERENCES

- 1 A. Ohtomo and H. Y. Hwang, *Nature* **427**, 423 (2004).
- 2 N. Reyren, S. Thiel, A. D. Caviglia, L. F. Kourkoutis, G. Hammerl, C. Richter, C. W. Schneider, T. Kopp, A.-S. Ruetschi, D. Jaccard, M. Gabay, D. A. Muller, J.-M. Triscone, and J. Mannhart, *Science* **317**, 1196 (2007).
- 3 K. Ueno, S. Nakamura, H. Shimotani, A. Ohtomo, N. Kimura, T. Nojima, H. Aoki, Y. Iwasa, and M. Kawasaki, *Nat. Mater.* **7**, 855 (2008).
- 4 A. Brinkman, M. Huijben, M. van Zalk, J. Huijben, U. Zeitler, J. C. Maan, W. G. van der Wiel, G. Rijnders, D. H. A. Blank, and H. Hilgenkamp, *Nat. Mater.* **6**, 493 (2007).
- 5 A. D. Caviglia, S. Gariglio, C. Cancellieri, B. Sacépé, A. Fête, N. Reyren, M. Gabay, A. F. Morpurgo, and J.-M. Triscone, *Phys. Rev. Lett.* **105**, 236802 (2010).
- 6 F. Trier, G. E. D. K. Prawiroatmodjo, Z. Zhong, D. V. Christensen, M. von Soosten, A. Bhowmik, J. M. G. Lastra, Y. Chen, T. S. Jespersen, and N. Pryds, *Phys. Rev. Lett.* **117**, 096804 (2016).
- 7 A. D. Caviglia, M. Gabay, S. Gariglio, N. Reyren, C. Cancellieri, and J.-M. Triscone, *Phys. Rev. Lett.* **104**, 126803 (2010).
- 8 E. Lesne, Y. Fu, S. Oyarzun, J. C. Rojas-Sánchez, D. C. Vaz, H. Naganuma, G. Sicoli, J.-P. Attané, M. Jamet, E. Jacquet, J.-M. George, A. Barthélémy, H. Jaffrès, A. Fert, M. Bibes, and L. Vila, *Nat. Mater.* **15**, 1261 (2016).
- 9 Q. Song, H. Zhang, T. Su, W. Yuan, Y. Chen, W. Xing, J. Shi, J. Sun, and W. Han, *Sci. Adv.* **3**, e1602312 (2017).
- 10 Y. Wang, R. Ramaswamy, M. Motapothula, K. Narayanapillai, D. Zhu, J. Yu, T. Venkatesan, and H. Yang, *Nano Lett.* **17**, 7659 (2017).
- 11 D. C. Vaz, P. Noël, A. Johansson, B. Göbel, F. Y. Bruno, G. Singh, S. McKeown-Walker, F. Trier, L. M. Vicente-Arche, A. Sander, S. Valencia, P. Bruneel, M. Vivek, M. Gabay, N. Bergeal, F. Baumberger, H. Okuno, A. Barthélémy, A. Fert, L. Vila, I. Mertig, J.-P. Attané, and M. Bibes, *Nat. Mater.* **18**, 1187 (2019).
- 12 S. Ohya, D. Araki, L. D. Anh, S. Kaneta, M. Seki, H. Tabata, and M. Tanaka, *Phys. Rev. Res.* **2**, 012014 (2020).
- 13 P. Noël, F. Trier, L. M. Vicente Arche, J. Bréhin, D. C. Vaz, V. Garcia, S. Fusil, A. Barthélémy, L. Vila, M. Bibes, and J.-P. Attané, *Nature* **580**, 483 (2020).
- 14 Y. A. Bychkov and E. I. Rashba, *JETP Lett.* **39**, 78 (1984).
- 15 A. Manchon, H. C. Koo, J. Nitta, S. M. Frolov, and R. A. Duine, *Nat. Mater.* **14**, 871 (2015).
- 16 I. Mihai Miron, G. Gaudin, S. Auffret, B. Rodmacq, A. Schuhl, S. Pizzini, J. Vogel, and P. Gambardella, *Nat. Mater.* **9**, 230 (2010).
- 17 L. Liu, C.-F. Pai, Y. Li, H. W. Tseng, D. C. Ralph, and R. A. Buhrman, *Science* **336**, 555 (2012).
- 18 Z. Luo, A. Hrabec, T. P. Dao, G. Sala, S. Finizio, J. Feng, S. Mayr, J. Raabe, P. Gambardella, and L. J. Heyderman, *Nature* **579**, 214 (2020).
- 19 H. Lee, N. Campbell, J. Lee, T. J. Asel, T. R. Paudel, H. Zhou, J. W. Lee, B. Noesges, J. Seo, B. Park, L. J. Brillson, S. H. Oh, E. Y. Tsybmal, M. S. Rzchowski, and C. B. Eom, *Nat. Mater.* **17**, 231 (2018).
- 20 L. D. Anh, S. Kaneta, M. Tokunaga, M. Seki, H. Tabata, M. Tanaka, and S. Ohya, *Adv. Mater.* **32**, 1906003 (2020).
- 21 B. Dieny and M. Chshiev, *Rev. Mod. Phys.* **89**, 025008 (2017).
- 22 S. Nakazawa, A. Obinata, D. Chiba, and K. Ueno, *Appl. Phys. Lett.* **110**, 062406 (2017).
- 23 T. Seki, M. Tsujikawa, K. Ito, K. Uchida, H. Kurebayashi, M. Shirai, and K. Takanashi, *Phys. Rev. Mater.* **4**, 064413 (2020).
- 24 Z. Zhang, Z. Li, K. Meng, Y. Wu, J. Chen, X. Xu, and Y. Jiang, *Appl. Phys. Lett.* **116**, 232402 (2020).
- 25 M. Kasai and H. Dohi, *Surf. Sci.* **666**, 14 (2017).
- 26 J. Sinova, S. O. Valenzuela, J. Wunderlich, C. H. Back, and T. Jungwirth, *Rev. Mod. Phys.* **87**, 1213 (2015).
- 27 Y. Du, H. Gamou, S. Takahashi, S. Karube, M. Kohda, and J. Nitta, *Phys. Rev. Appl.* **13**, 054014 (2020).
- 28 H. Zhou, P. Wochner, A. Schöps, and T. Wagner, *J. Cryst. Growth* **234**, 561 (2002).
- 29 L. Vitos, A. V. Ruban, H. L. Skriver, and J. Kollár, *Surf. Sci.* **411**, 186 (1998).
- 30 N. Nakajima, T. Koide, T. Shidara, H. Miyauchi, H. Fukutani, A. Fujimori, K. Iio, T. Katayama, M. Nývlt, and Y. Suzuki, *Phys. Rev. Lett.* **81**, 5229 (1998).
- 31 S. Monso, B. Rodmacq, S. Auffret, G. Casali, F. Fettar, B. Gilles, B. Dieny, and P. Boyer, *Appl. Phys. Lett.* **80**, 4157 (2002).
- 32 A. Manchon, C. Ducruet, L. Lombard, S. Auffret, B. Rodmacq, B. Dieny, S. Pizzini, J. Vogel, V. Uhlir, M. Hochstrasser, and G. Panaccione, *J. Appl. Phys.* **104**, 043914 (2008).

- ³³C. Nistor, T. Balashov, J. J. Kavich, A. Lodi Rizzini, B. Ballesteros, G. Gaudin, S. Auffret, B. Rodmacq, S. S. Dhesi, and P. Gambardella, *Phys. Rev. B* **84**, 054464 (2011).
- ³⁴P. Bruno, *Phys. Rev. B* **39**, 865 (1989).
- ³⁵I. I. Oleinik, E. Y. Tsymbal, and D. G. Pettifor, *Phys. Rev. B* **62**, 3952 (2000).
- ³⁶H. K. Gweon, S. J. Yun, and S. H. Lim, *Sci. Rep.* **8**, 1266 (2018).
- ³⁷H. X. Yang, M. Chshiev, B. Dieny, J. H. Lee, A. Manchon, and K. H. Shin, *Phys. Rev. B* **84**, 054401 (2011).
- ³⁸P. F. Garcia, *J. Appl. Phys.* **63**, 5066 (1988).
- ³⁹B. D. Hermsmeier, R. F. C. Farrow, C. H. Lee, E. E. Marinero, C. J. Lin, R. F. Marks, and C. J. Chien, *J. Appl. Phys.* **69**, 5646 (1991).